

Supporting Information for

**Structural Evolution of Ag-Pd Bimetallic Nanoparticles through
Controlled Galvanic Replacement: Effects of Mild Reducing Agents**

Hao Jing and Hui Wang*

*Department of Chemistry and Biochemistry, University of South Carolina, Columbia,
South Carolina 29208, United States*

* To whom correspondence should be addressed.

Email: wang344@mailbox.sc.edu; Phone: 803-777-2203; Fax: 803-777-9521.

S1. Additional Experimental Details

Synthesis of Ag Nanocubes. To fabricate Ag nanocubes (~ 40 nm edge-length), 40 mL of ethylene glycol (EG) was added into a 100 mL round bottom flask and preheated under magnetic stir in an oil bath set to 150°C for about 40 min. Then 500 μL of 3 mM NaHS solution, 3 mL of 3 mM HCl, and 10 mL of PVP (100 mg/mL) were added sequentially. After stirring the mixture for 2 min, 3 mL of 282 mM CF_3COOAg solution was added. During the entire process, the flask was capped with a glass stopper except during the addition of reagents. After 22 min, the reaction was quenched in an ice-water bath when the suspension had reached a brown color with a characteristic plasmon resonance peak at ~ 420 nm in the extinction spectrum. The Ag nanocubes were centrifuged (8000 rpm, 8 min), washed with acetone and then water, and finally redispersed in 6 mL of EG. The particle concentration of the 40 nm nanocubes was 2.5×10^{12} particles mL^{-1} . Ag nanocubes with average edge-length of ~ 100 nm were prepared through a seed-mediated growth process. Typically, 10 mL of EG was added into a 50 mL round bottom flask and heated in an oil bath at 150°C under magnetic stir. After 10 min, 3 mL of PVP (250 mg/mL in EG) was added. After another 10 min, 200 μL of colloidal suspension of ~ 40 nm Ag nanocubes was introduced, followed by the addition of 2 mL of 282 mM AgNO_3 . After 20 min, the reaction was quenched by immersing the reaction mixture in an ice-water bath. The product was centrifuged (8000 rpm, 8 min), washed with acetone and then water, and finally redispersed in 10 mL of water for future use. The particle concentration of the ~ 100 nm nanocubes was 5×10^{10} particles mL^{-1} .

Synthesis of Quasi-Spherical Ag Nanoparticles. Single-crystalline Ag quasi-spherical nanoparticles were fabricated through etching of Ag nanocubes by $\text{Fe}(\text{NO}_3)_3$. 200 μL of aqueous solution of Ag nanocubes (100 nm edge-length) was added to 2 mL of ultrapure water in a small vial under magnetic stir. The etching was initiated by the addition of 20 μL of 50 mM freshly-prepared $\text{Fe}(\text{NO}_3)_3$ at room temperature and the sample was centrifuged (6000 rpm, 5min) after 20 min and was redispersed in 1 mL water to obtain Ag nanocubes with truncated corners. To obtain Ag quasi-spherical nanoparticles, the protocol was similar to that used for the truncated nanocubes except for the use of 5 μL of 500 mM freshly-prepared $\text{Fe}(\text{NO}_3)_3$ solution as the etchant. The vial was capped at room temperature for 2 hours till the completion of etching. The resulting Ag quasi-spherical nanoparticles were centrifuged (6000 rpm, 5min), washed with water twice, and finally redispersed in 1 mL water.

Synthesis of Quasi-Spherical Au Nanoparticles. Quasi-spherical Au nanoparticles with average diameter of ~ 94 nm were synthesized by reducing chloroauric acid with formaldehyde at room temperature. Briefly, 50 mg of K_2CO_3 was dissolved in 200 mL water, followed by the addition of 3 mL of 25 mM HAuCl_4 . The mixture was aged in the dark for at least 12 h. Then 0.3 mL of formaldehyde solution (37 wt%) was added into the mixture under vigorous magnetic stir at 300 rpm. A brick-red colloidal suspension began to form after ~ 15 min. The colloidal suspension was kept being stirred for 30 min. Then Au nanoparticles were centrifuged at 2000 rpm, washed with PVP aqueous solution (20 g/L) and ethanol in sequence, and finally redispersed in 10 mL of water. The final concentration of aqueous Au colloidal suspension was $\sim 6 \times 10^{10}$ particles mL^{-1} .

S2. Additional Figures

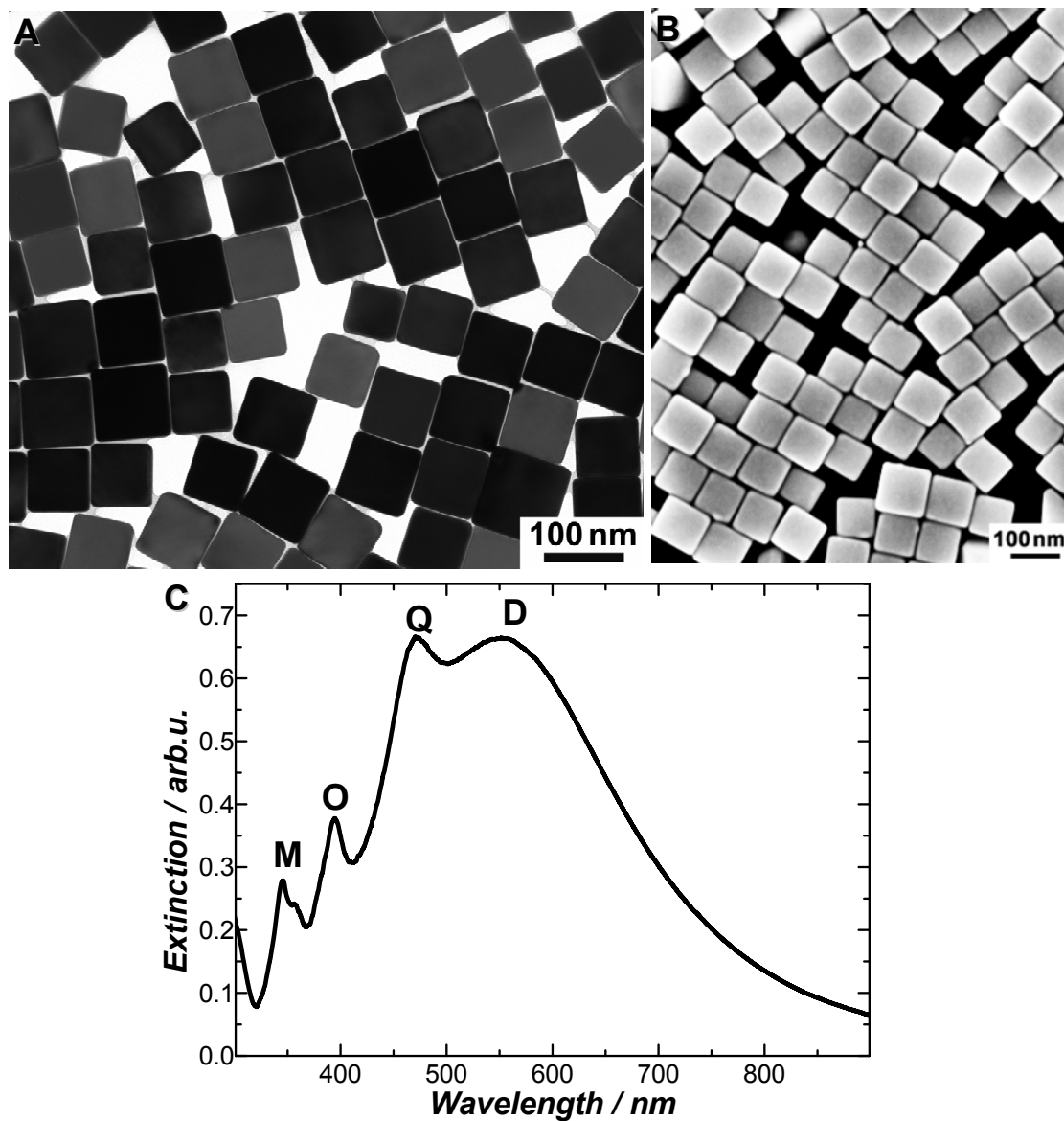


Figure S1. (A) TEM and (B) SEM images of Ag nanocubes. (C) Extinction spectrum of colloidal Ag nanocubes dispersed in H₂O. The four extinction peaks were assigned to the dipole, quadrupole, octupole, and higher-order multipole plasmon resonances, which were labeled as D, Q, O, and M respectively.

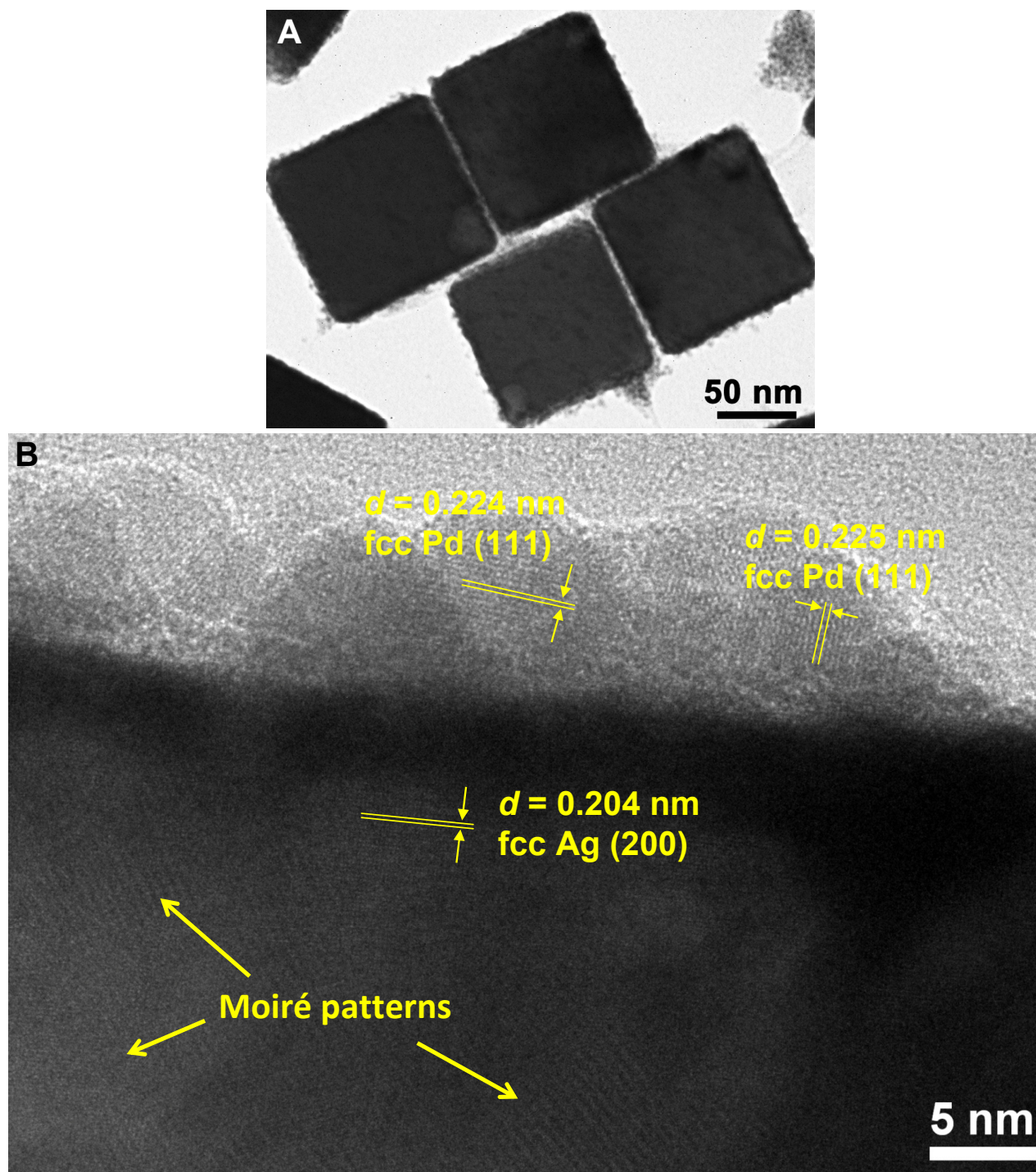


Figure S2. (A) TEM image showing the initiation of pitting and deposition of Pd on the outer surfaces of Ag nanocubes upon galvanic replacement of Ag nanocubes with 20 μL of 1 mM H_2PdCl_4 in the absence of reducing agents. (B) High-resolution TEM image showing the surface structures of one particle.

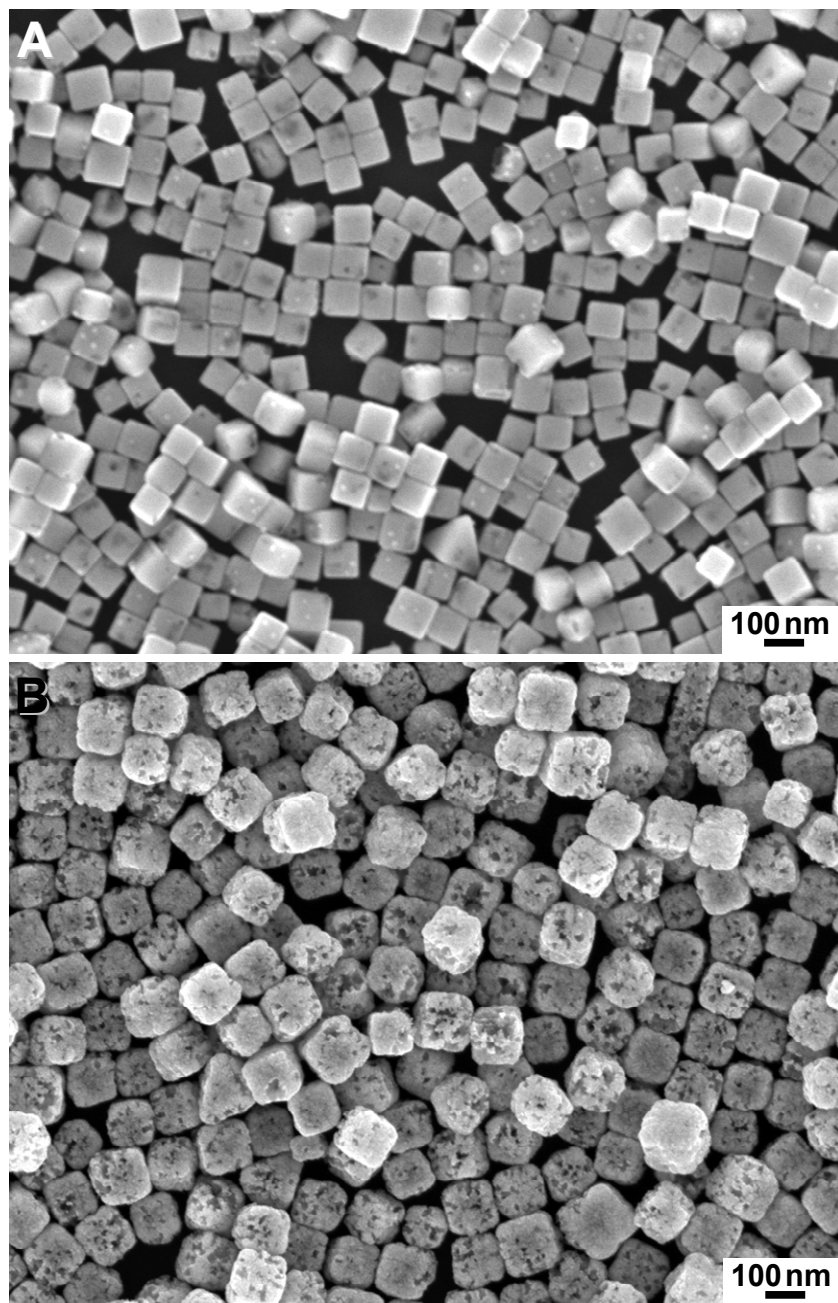


Figure S3. SEM images of Ag-Pd bimetallic nanoparticles obtained through galvanic replacement of Ag nanocubes with (A) 60 μL and (B) 200 μL of 1 mM H_2PdCl_4 in the absence of reducing agents.

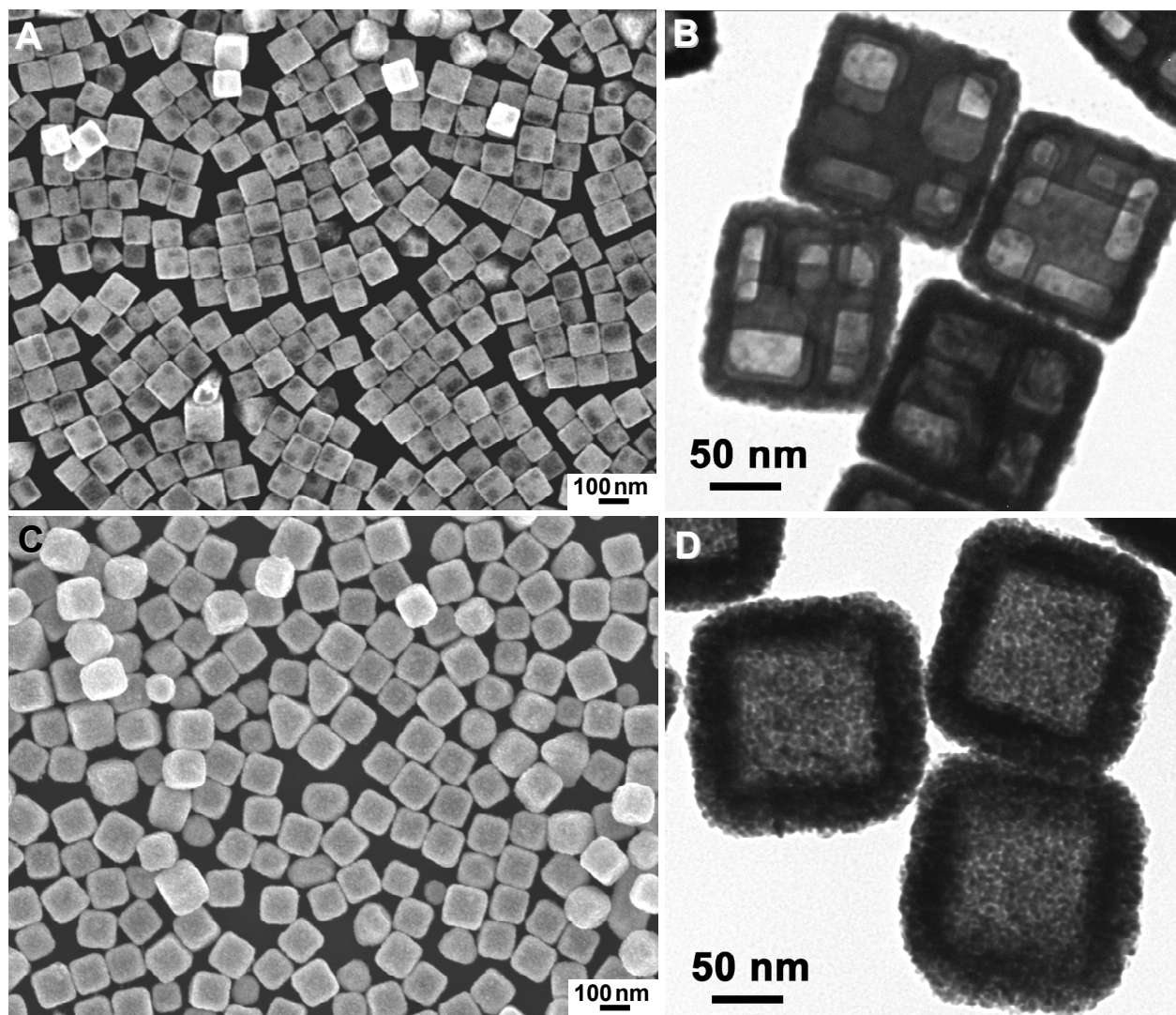


Figure S4. (A) SEM and (B) TEM images of Ag-Pd multi-chambered nanoboxes obtained through galvanic replacement of Ag nanocubes with 60 μL of 1 mM H_2PdCl_4 in the presence of AA. (C) SEM and (D) TEM images of Ag-Pd hollow nanoparticles with porous walls obtained through galvanic replacement of Ag nanocubes with 200 μL of 1 mM H_2PdCl_4 in the presence of AA.

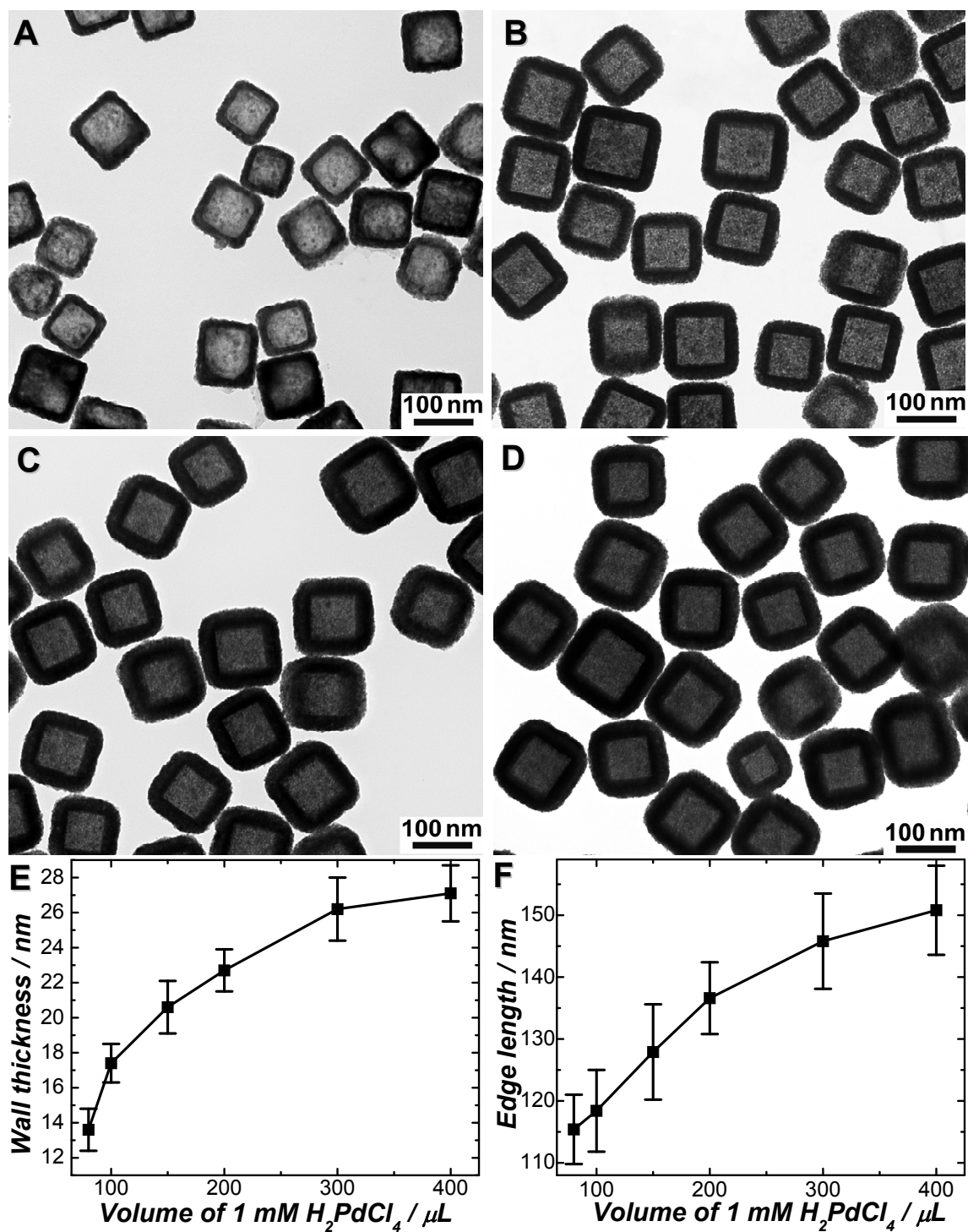


Figure S5. TEM images of Ag-Pd bimetallic hollow nanostructures obtained through galvanic replacement of Ag nanocubes with (A) 80 μL , (B) 150 μL , (C) 300 μL , and (D) 400 μL of 1 mM H_2PdCl_4 solution in the presence of AA. (E) Average wall thickness and (F) edge length of Ag-Pd bimetallic hollow nanoparticles as a function of the volume of 1 mM H_2PdCl_4 . The error bars represent the standard deviations obtained from more than 200 nanoparticles in the TEM image of each sample.

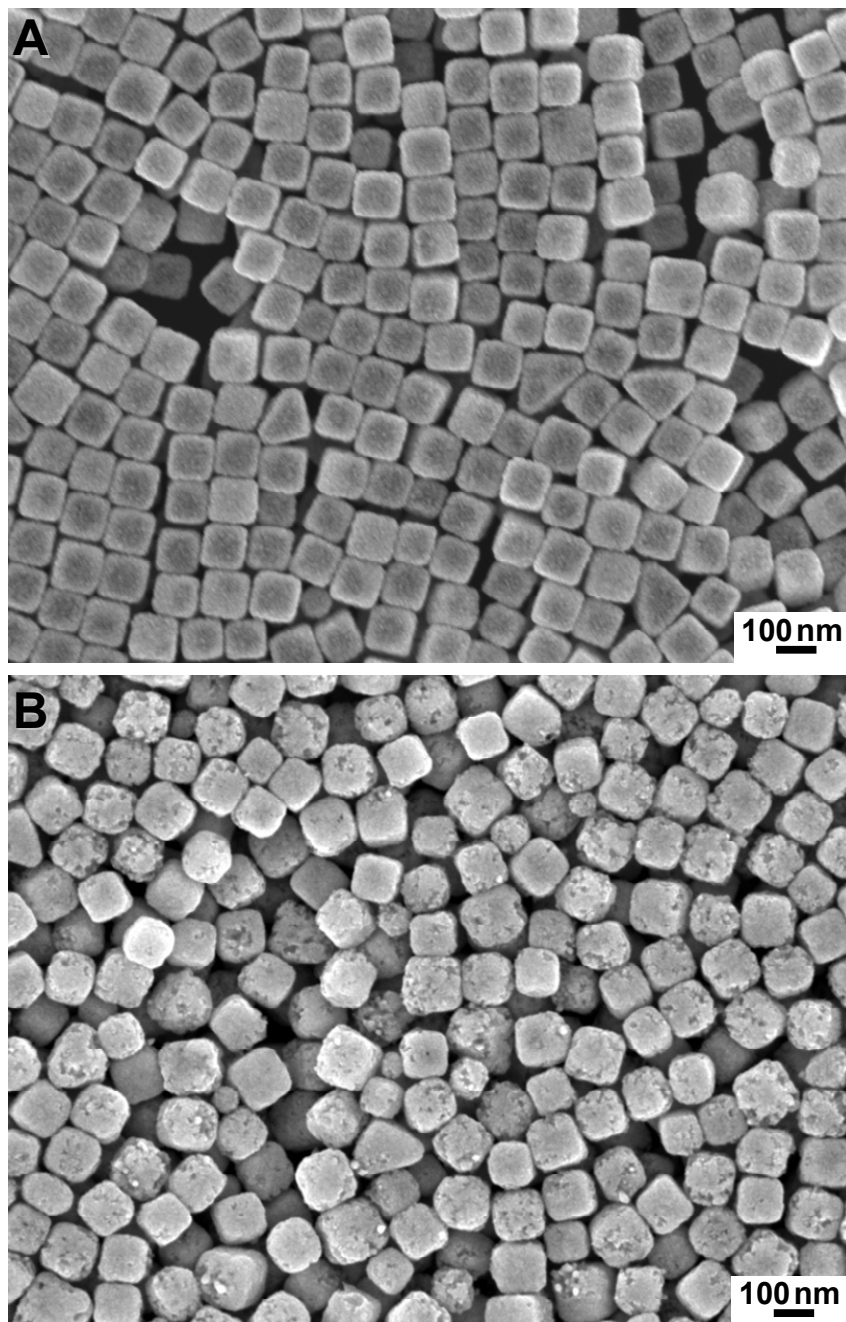


Figure S6. SEM images of Ag-Pd bimetallic nanoparticles obtained through galvanic replacement of Ag nanocubes with (A) 60 μL and (B) 200 μL of 1 mM H_2PdCl_4 in the presence of HCHO.

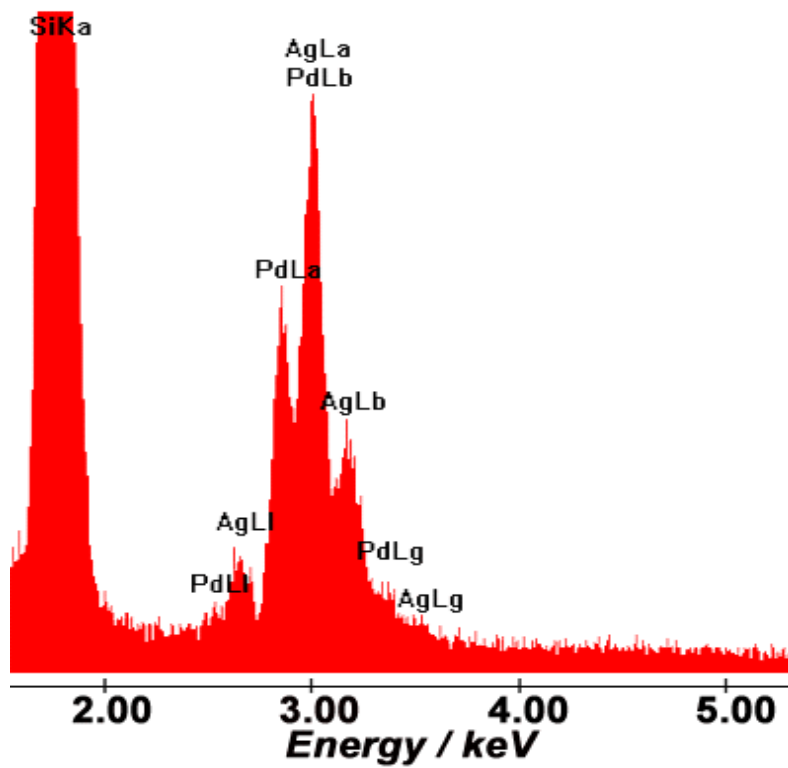


Figure S7. EDS spectrum of Ag-Pd bimetallic nanoparticles obtained through galvanic replacement of Ag nanocubes with 400 μL of 1 mM H_2PdCl_4 in the presence of AA.

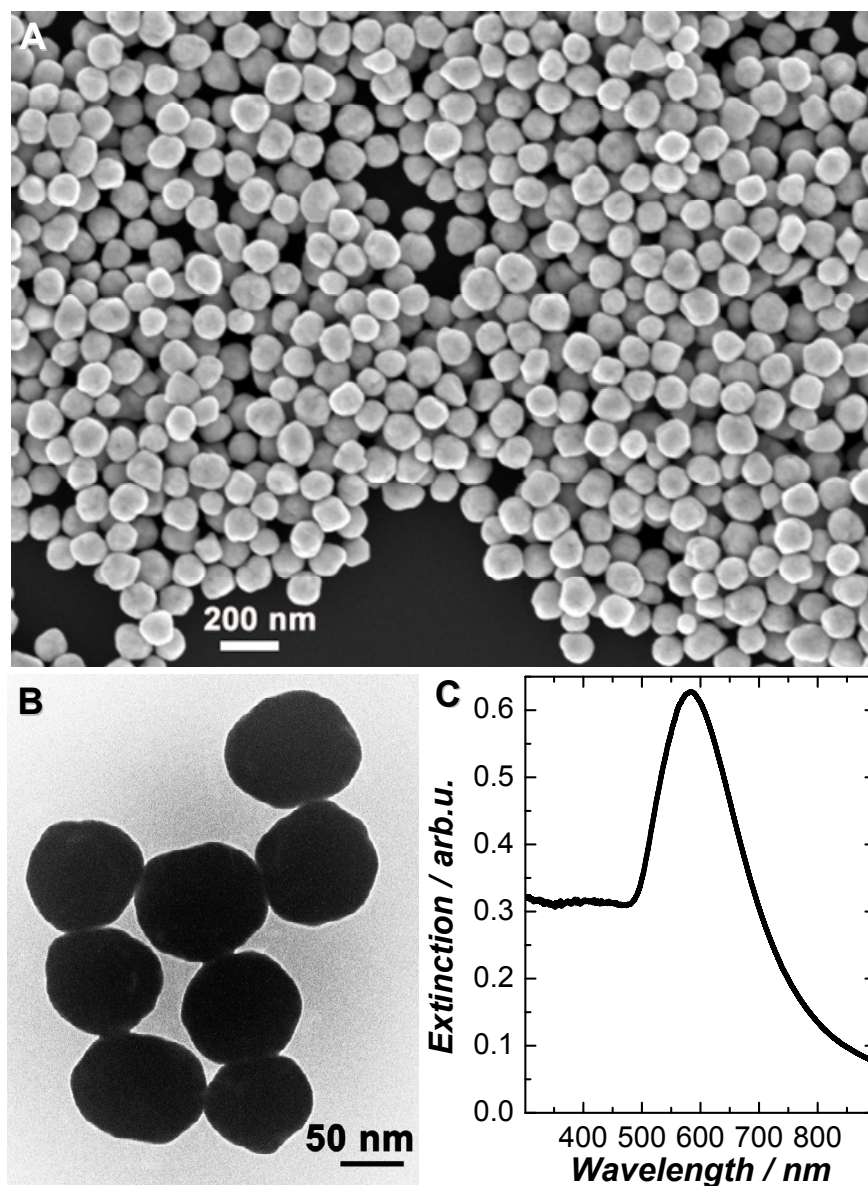


Figure S8. (A) SEM image, (B) TEM image, and (C) extinction spectrum of Au quasi-spherical nanoparticles.

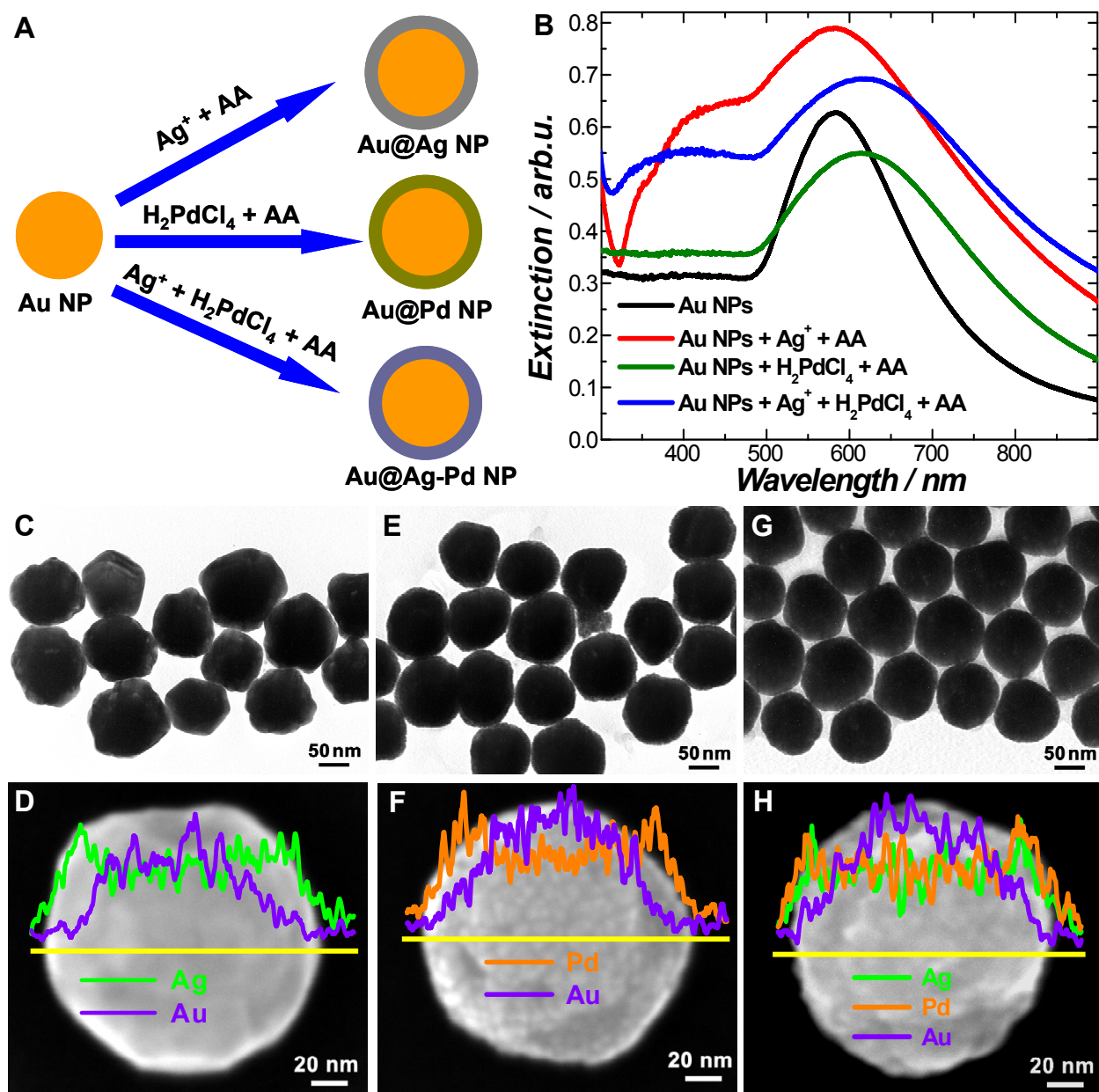


Figure S9. (A) Schematic illustration of Au nanoparticle-seeded electroless plating of Ag and Pd in the presence of AA. (B) Extinction spectra of Au nanoparticles and Au@Ag, Au@Pd, and Au@Ag-Pd alloy core-shell nanoparticles. TEM images of (C) Au@Ag, (E) Au@Pd, and (G) Au@Ag-Pd alloy core-shell nanoparticles. SEM images and EDS line-scan elemental analysis of individual (D) Au@Ag, (F) Au@Pd, and (H) Au@Ag-Pd core-shell nanoparticles.

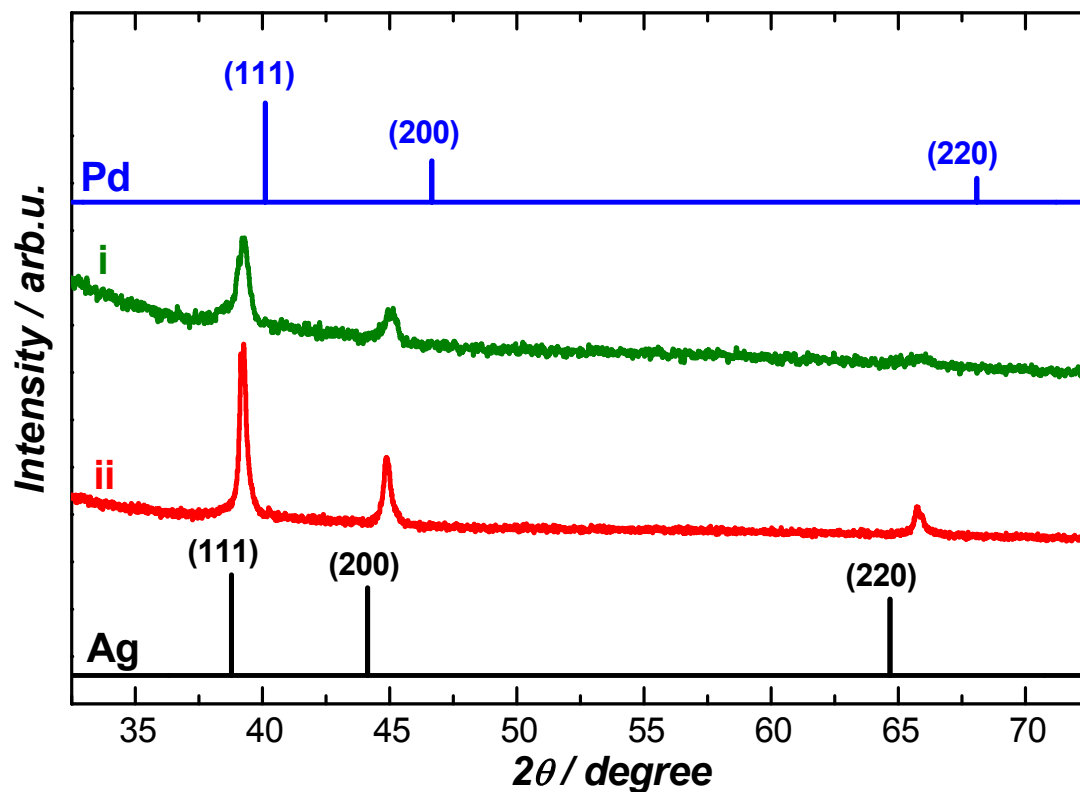


Figure S10. PXRD patterns of Ag-Pd bimetallic hollow nanoparticles obtained through galvanic replacement of Ag nanocubes with (i) 200 μL of 1 mM H_2PdCl_4 in the presence of AA and (ii) 200 μL of 1 mM H_2PdCl_4 in the presence of HCHO. The standard PXRD patterns for bulk face-centered cubic Ag (PDF number 3-391) and Pd (PDF number 5-681) are also included for comparison.

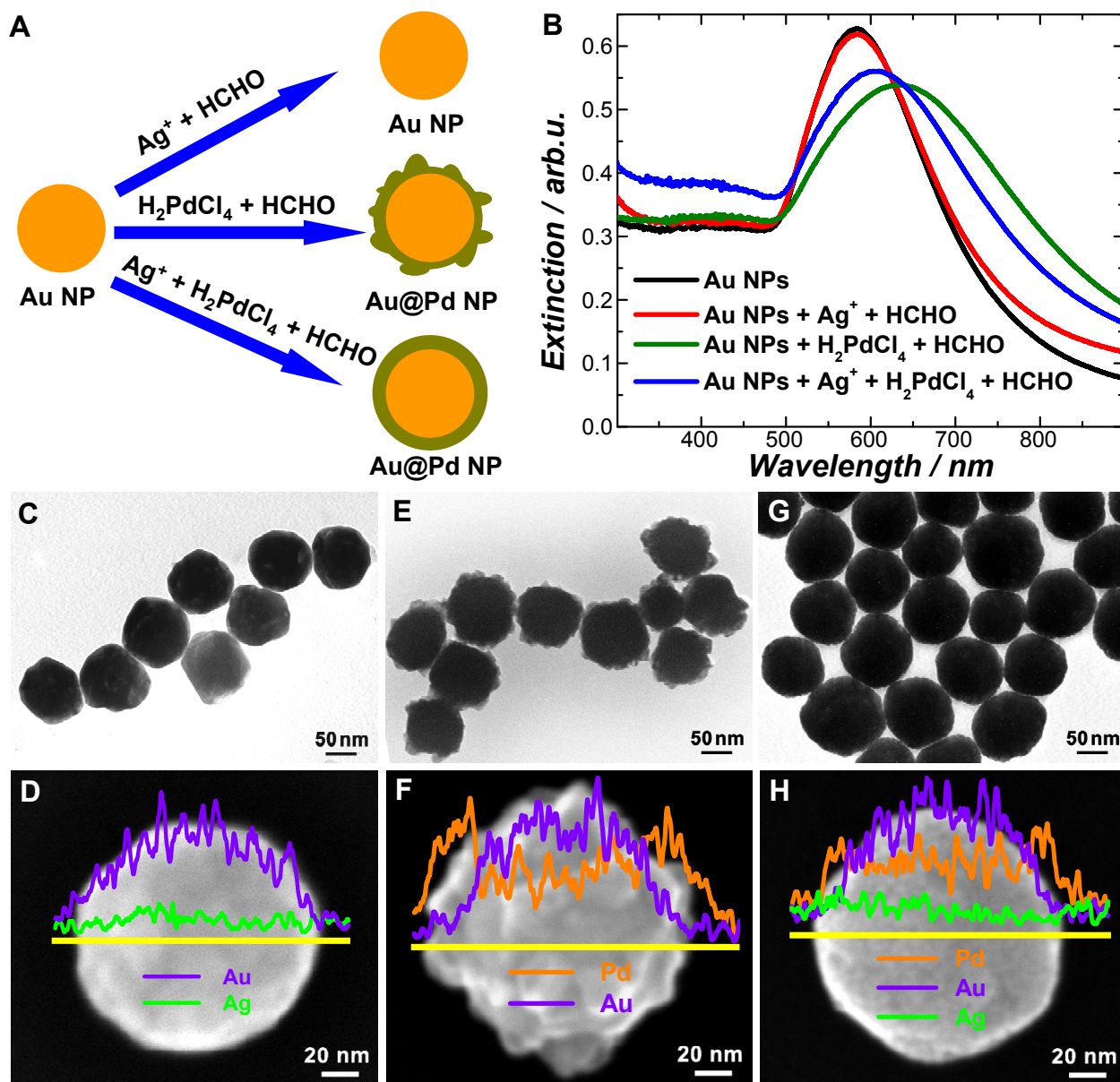


Figure S11. (A) Schematic illustration of Au nanoparticle-seeded electroless plating of Ag and Pd in the presence of HCHO. (B) Extinction spectra of Au nanoparticles and the nanoparticles synthesized by the Au-seeded reduction of Ag^+ , H_2PdCl_4 , and $\text{Ag}^+/\text{H}_2\text{PdCl}_4$ with HCHO. (C) TEM image and (D) SEM image with EDS results of nanoparticles synthesized by Au-seeded reduction of Ag^+ with HCHO. (E) TEM image and (F) SEM image with EDS results of the nanoparticles synthesized by Au-seeded reduction of H_2PdCl_4 with HCHO. (G) TEM image and (H) SEM image with EDS results of nanoparticles synthesized by the Au-seeded reduction of co-existing Ag^+ and H_2PdCl_4 with HCHO.

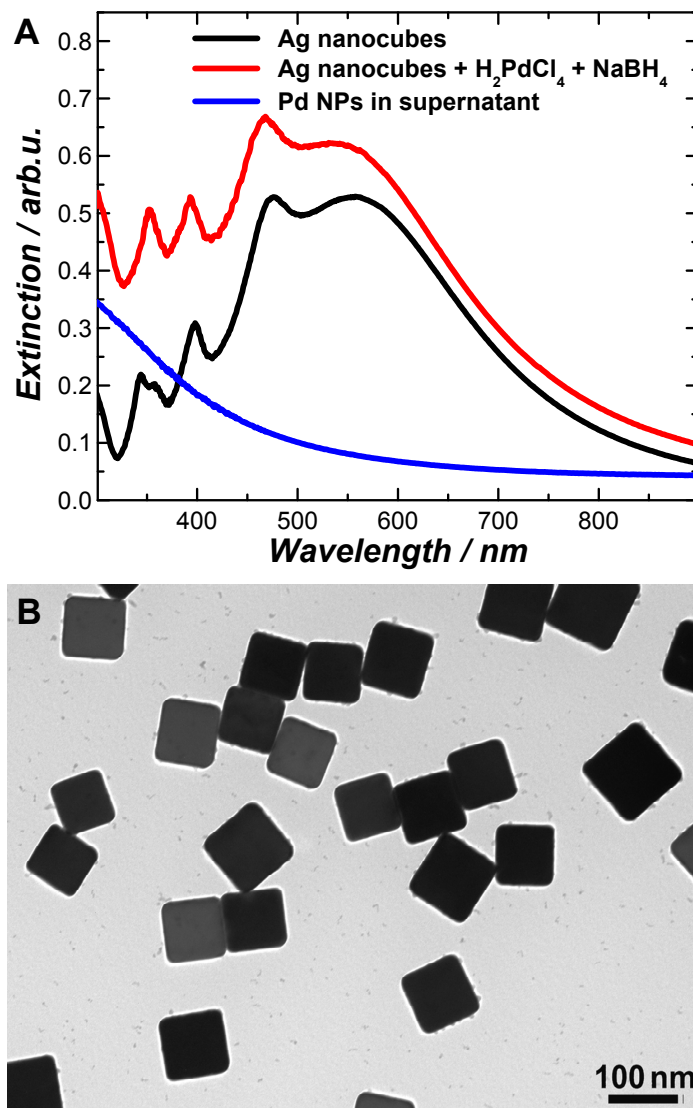


Figure S12. (A) Extinction spectra of Ag nanocubes, the colloidal sample obtained upon reacting 30 μL of Ag nanocubes (5×10^{10} particle mL^{-1}) with 100 μL of 1 mM H_2PdCl_4 and 50 μL of 50 mM NaBH_4 , and the Pd nanoparticles remaining in the supernatant after the Ag nanocubes were centrifuged. (B) TEM image of a mixture of Ag nanocubes and Pd nanoparticles (2-3 nm in size) obtained upon reacting 30 μL of Ag nanocubes (5×10^{10} particle mL^{-1}) with 100 μL of 1 mM H_2PdCl_4 and 50 μL of 50 mM NaBH_4 .

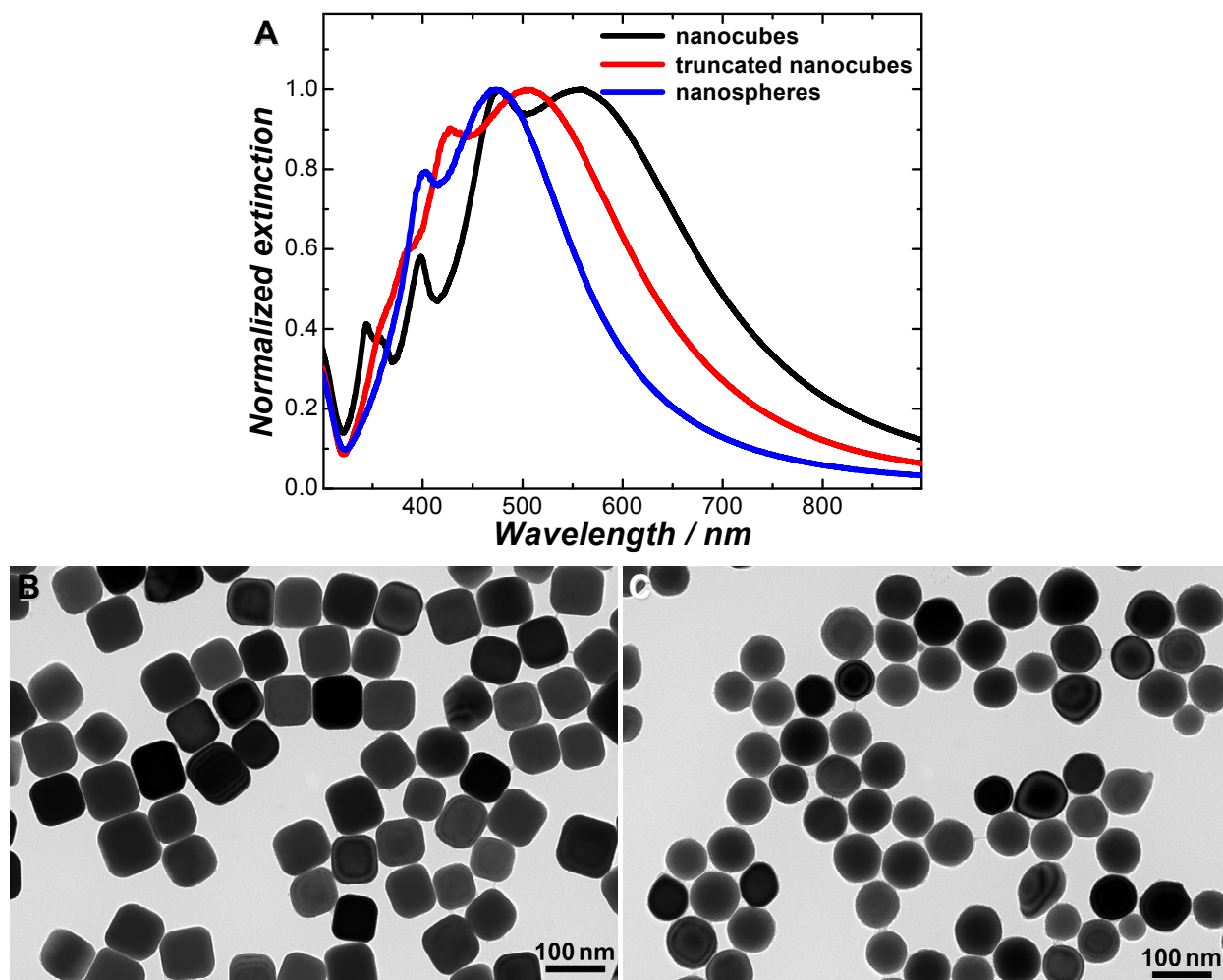


Figure S13. (A) Extinction spectra of Ag nanocubes, truncated Ag nanocubes, and Ag quasi-spherical nanoparticles obtained through $\text{Fe}(\text{NO}_3)_3$ etching. The truncated Ag nanocubes were obtained by etching Ag nanocubes with 20 μL of 50 mM $\text{Fe}(\text{NO}_3)_3$ solution for 20 min at room temperature. The Ag quasi-spherical nanoparticles were obtained by etching Ag nanocubes with 5 μL of 500 mM $\text{Fe}(\text{NO}_3)_3$ solution for 2 hrs at room temperature. TEM images of (B) truncated Ag nanocubes and (C) Ag quasi-spherical nanoparticles.

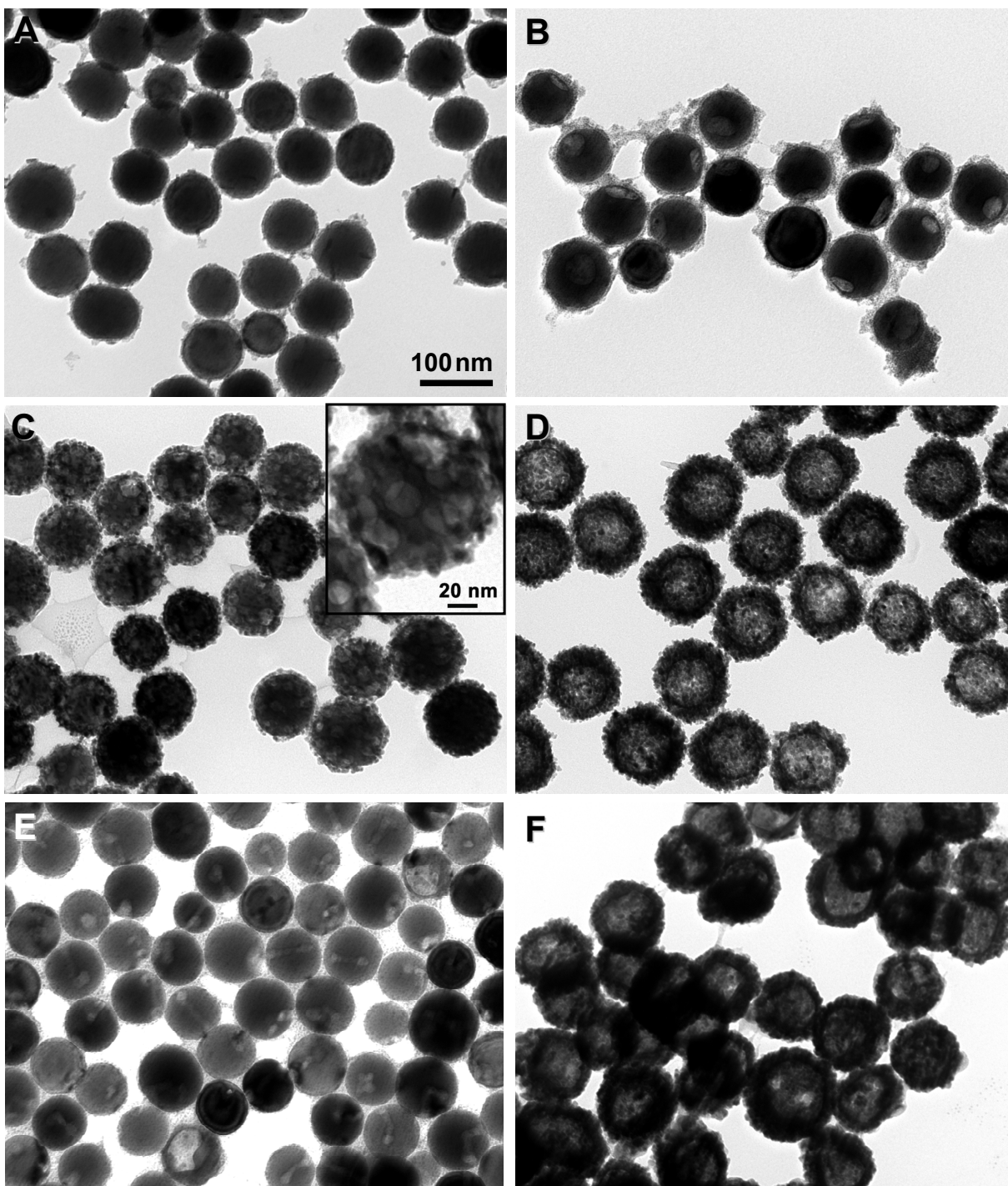


Figure S14. TEM images of Ag-Pd bimetallic hollow nanostructures obtained through galvanic replacement between Ag quasi-spherical nanoparticles and H_2PdCl_4 under various conditions: (A) 15 μL of 1 mM H_2PdCl_4 , without reducing agent; (B) 60 μL of 1 mM H_2PdCl_4 , without reducing agent; (C) 15 μL of 1 mM H_2PdCl_4 , with AA; (D) 60 μL of 1 mM H_2PdCl_4 , with AA; (E) 15 μL of 1 mM H_2PdCl_4 , with HCHO; (F) 60 μL of 1 mM H_2PdCl_4 , with HCHO. The inset in panel C shows the TEM image of one multi-chambered Ag-Pd bimetallic nanoshell. All TEM images share the same scale bar in panel A.

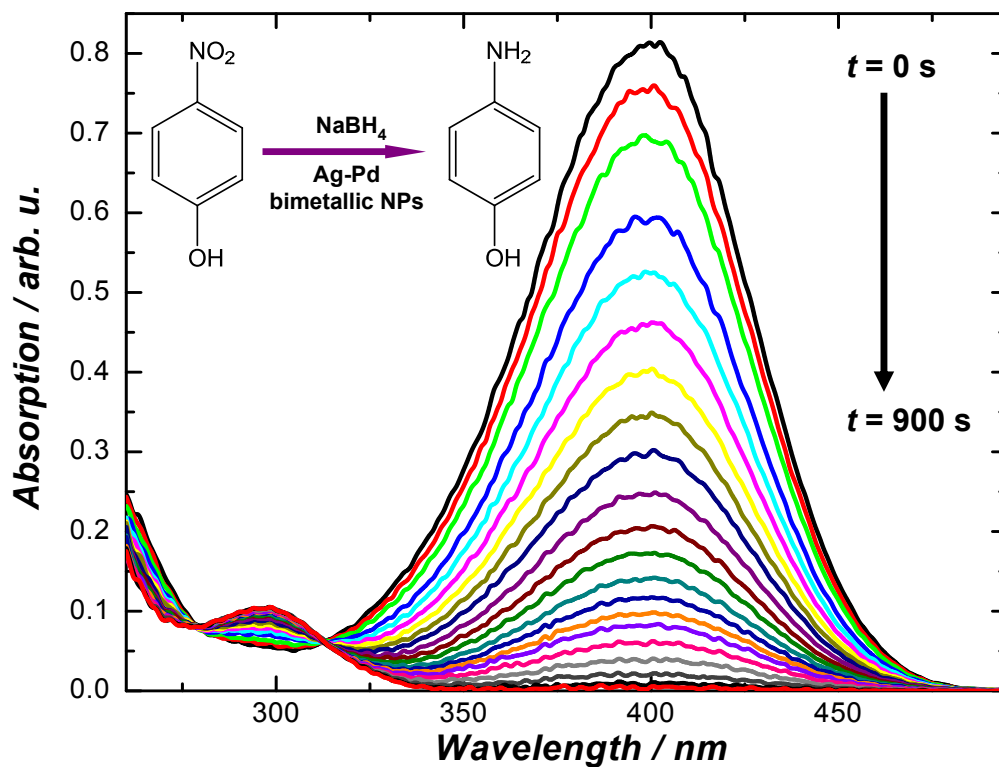


Figure S15. Time-resolved UV-vis absorption spectra of the reaction mixture during the Ag-Pd bimetallic nanoparticle-catalyzed hydrogenation of p-nitrophenol. The time interval between two consecutive spectra was 25 s. The Ag-Pd bimetallic nanoparticles were synthesized by galvanic replacement of Ag nanocubes with 100 μL of 1 mM H_2PdCl_4 in the presence of AA. The extinctions of the nanoparticles were subtracted from the overall extinctions.